Structural Similarities between the N-Terminal Domain of *Clostridium pasteurianum* Hydrogenase and Plant-Type Ferredoxins

Rainer Kümmerle,[‡] Mohamed Atta,[§] Johann Scuiller,[‡] Jacques Gaillard,[‡] and Jacques Meyer*[,§]

Département de Biologie Moléculaire et Structurale, CEA-Grenoble, 38054 Grenoble, France, and Département de Recherche Fondamentale sur la Matière Condensée, Service de Chimie Inorganique et Biologique, CEA-Grenoble, 38054 Grenoble, France

Received October 12, 1998; Revised Manuscript Received November 30, 1998

ABSTRACT: An N-terminal domain of *Clostridium pasteurianum* hydrogenase I, encompassing 76 residues out of the 574 composing the full-size enzyme, had previously been overproduced in *Escherichia coli* and shown to form a stable fold around a [2Fe-2S] cluster. This domain displays only marginal sequence similarity with [2Fe-2S] proteins of known structure, and therefore, two-dimensional ^{1}H NMR has been implemented to elucidate features of the polypeptide fold. Despite the perturbing presence of the paramagnetic [2Fe-2S] cluster, 57 spin systems were detected in the TOCSY spectra, 52 of which were sequentially assigned through NOE connectivities. Several secondary structure elements were identified. The N terminus of the protein consists of two antiparallel β strands followed by an α helix contacting both strands. Two additional antiparallel β strands, one of them at the C terminus of the sequence, form a four-stranded β sheet together with the two N-terminal strands. The proton resonances that can be attributed to this $\beta 2\alpha\beta 2$ structural motif undergo no paramagnetic perturbations, suggesting that it is distant from the [2Fe-2S] cluster. In plant- and mammalian-type ferredoxins, a very similar structural pattern is found in the part of the protein farthest from the [2Fe-2S] cluster. This indicates that the N-terminal domain of *C. pasteurianum* hydrogenase folds in a manner very similar to those of plant- and mammalian-type ferredoxins over a significant part (ca. 50%) of its structure. Even in the vicinity of the metal site, where ^{1}H NMR data are blurred by paramagnetic interactions, the N-terminal domains of hydrogenase and mammalian- and plant-type ferredoxins most likely display significant structural similarity, as inferred from local sequence alignments and from previously reported circular dichroism and resonance Raman spectra. These data afford structural information on a kind of [2Fe-2S] cluster-containing domain that occurs in a number of redox enzymes and complexes. In addition, together with previously published sequence alignments, they highlight the widespread distribution of the plant-type ferredoxin fold in bioenergetic systems encompassing anaerobic metabolism, photosynthesis, and aerobic respiratory chains.

Hydrogenases that contain iron only, or [Fe]-hydrogenases, are found in a variety of anaerobic bacteria and protozoa (*1*−*4*). These enzymes are diverse in quaternary structure (one to four subunits) but share a catalytic subunit composed of 420−580 amino acids (*1*, *2*). The sequences of the latter polypeptide chains appear to be composed of discrete sections. A C-terminal domain of 320−350 amino acids that is likely to accommodate the hydrogen-activating site, and, neighboring the latter, an 80−100-residue domain homologous to 2[4Fe-4S] ferredoxins, are both present in all [Fe]-hydrogenases (*2*, *5*). An additional N-terminal domain occurs in only some of these enzymes, e.g., *Clostridium pasteurianum* hydrogenase I. This nonconserved N-terminal section of 120−130 residues is believed to contain two Fe−S clusters, although it displays no canonic cysteine-containing sequence pattern (*2*). We have recently expressed in *Escherichia coli* a fragment of the *C. pasteurianum* hydrogenase gene encoding the N-terminal half (residues 1−76) of the nonconserved N-terminal section of the primary structure (*5*). This polypeptide was shown to form a stable fold around a [2Fe-2S] cluster, probably in a manner very similar to that in the full-size enzyme. This new [2Fe-2S]-containing protein domain elicits wide interest in bioenergetics since its primary structure is homologous to several sequences found in various redox enzymes and complexes. However, no significant sequence similarities with proteins of known structure were detected. We have therefore carried out a two-dimensional (2D) NMR[1] investigation aimed at elucidating structural features of the N-terminal domain of *C. pasteurianum* hydrogenase.

MATERIALS AND METHODS

The N-terminal domain (HN76) of *C. pasteurianum* hydrogenase, as well as a variant having cysteine 39 replaced

* To whom correspondence should be addressed: DBMS-Métalloprotéines, CEA-Grenoble, 38054 Grenoble, France. Fax: (33) 4 76 88 58 72. E-mail: jacques.meyer@cea.fr.

[‡] Service de Chimie Inorganique et Biologique, CEA-Grenoble.

[§] Département de Biologie Moléculaire et Structurale, CEA-Grenoble.

[1] Abbreviations: *Cp*, *Clostridium pasteurianum*; Fd, ferredoxin; HN76, N-terminal (residues 1−76) fragment of *C. pasteurianum* hydrogenase I; NMR, nuclear magnetic resonance; NOE, nuclear Overhauser effect; NOESY, NOE spectroscopy; TOCSY, total correlation spectroscopy; WT, wild type.

10.1021/bi982416j CCC: $18.00
Published on Web 01/20/1999

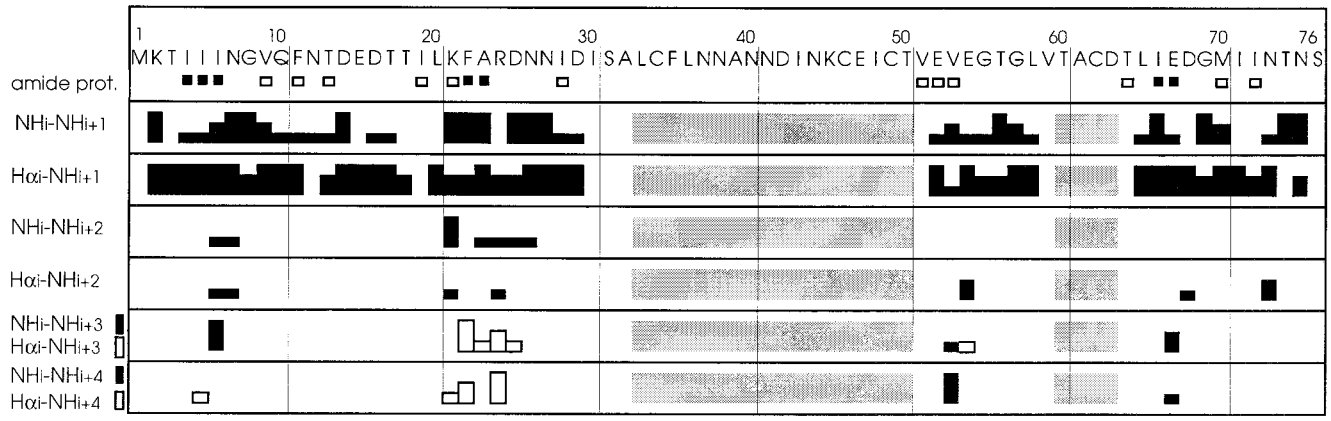

FIGURE 1: Sequential NOE connectivities of the HN76 protein. The line thickness increases with the strength of the NOE connectivities. No sequential NOEs were observed in the gray regions. The squares denote residues with slowly exchangeable amide protons: (□) exchange in 8−24 h and (■) exchange in more than 24 h.

with alanine (C39A), was prepared and purified as described previously (*5*). Most experiments were carried out with the C39A variant which is more stable than the wild-type protein. Since cysteine 39 is not a ligand of the [2Fe-2S] cluster (*5*), the structural changes resulting from this mutation were expected to be marginal. This has been confirmed by the close similarity of the NMR spectra of the wild-type and C39A proteins.

NMR samples contained 2.5−3 mM protein in 20 mM potassium phosphate (pH 7.5) and 0.1 M NaCl, with 10% D_2O (v/v) added as a spin lock signal. Samples for the measurements in D_2O were prepared by lyophilization of samples similar to those described above and subsequent dissolution in D_2O (99.8%, CEA-ORIS). An oxygen-free (<2 ppm) glovebox was implemented for the transfer of the samples into the NMR tubes, which were sealed with gastight screwcaps.

NMR experiments were performed on a Varian Unity Plus spectrometer operating at 500 MHz and using a reverse detection probe (*6*).

^{1}H NMR chemical shifts were referenced relative to the water signal resonance, set at 4.85 ppm at 293 K. Phase-sensitive TOCSY (*7*) and NOESY (*8*) experiments were performed at various temperatures between 290 and 298 K, in the pure absorption mode (*9*). The spin lock duration in TOCSY experiments was 40 ms, and mixing times in NOESY experiments were in the 30−170 ms range. The NMR data were processed on a Sun Sparc station with Varian software using the normal procedures for filtering the residual water signal, improving the resolution, or correcting the baseline (*6*).

RESULTS AND DISCUSSION

NMR Resonance Assignments. Amino acid spin systems were identified by their characteristic chemical shift patterns in the fingerprint region of the TOCSY spectra. The spin systems of 57 residues out of a total of 76 have been identified. This left out 19 residues for which the spin systems were not detected (table in the Supporting Information).

Sequence-specific assignments (*10*) were performed for 52 of the 57 observed spin systems, using αN, NN, and βN NOE connectivities (Figure 1). In this manner, four segments of the sequence (Lys2−Ile19, Lys21−Ala32, Val51−Val59, and Thr64−Ser76) could be traced in a straightforward manner. Ala39 was assigned by the presence of the relevant spin system in the spectra of the C39A variant, but not in those of the wild-type protein. Among the four unassigned spin systems, three were typical of aspartate or asparagine. Their resonances were broad and weak in the TOCSY spectra and disappeared altogether in the NOESY spectra, most probably due to the proximity of the [2Fe-2S] cluster. Any of the five asparagines (residues 37, 38, 40, 41, and 44) in the segment of residues 33−50 would be good candidates for these unassigned spin systems. Altogether, these observations are in keeping with previous work on other [2Fe-2S] proteins showing that relaxation broadening of the proton resonances by the paramagnetic Fe−S cluster impedes observation or assignment of 18−20 amino acid spin systems (*11*). As in previous reports (*11*−*15*), most of the non-observed amino acids occur in the vicinity of the cysteine ligands of the [2Fe-2S] cluster, residues 34, 46, 49, and 62 in this case. For instance, in the segment of residues 33−50, only the proton resonances of Ala39 could be assigned, by comparing the spectra of the wild-type and C39A proteins. Likewise, the spin systems of residues Ile48, Thr50, Thr60, Ala61, and Asp63 have remained unobserved (table in the Supporting Information). Paramagnetically shifted resonances that can be attributed to β protons of the cysteine ligands were detected as broad features in the 20−45 ppm range (not shown), in a fashion similar to that used with other [2Fe-2S] proteins (*16*).

Exchangeable Protons. Deuteron−proton exchange experiments (Figure 1) showed that 19 amide protons were slowly exchangeable. Seven of these (Ile4, Ile5, Ile6, Phe22, Ala23, Ile66, and Glu67) underwent limited exchange within 24 h, whereas 12 others (Val9, Phe11, Thr13, Ile19, Lys21, Ile28, Val51, Glu52, Val53, Thr64, Met70, and Ile72) exchanged over a period of 8−24 h. Most of these amide protons are involved in hydrogen bonds between secondary structure elements. The remaining slowly exchangeable amide protons are most probably not solvent accessible, and thereby provide information regarding the polypeptide fold (see below).

Secondary Structure. Analysis of the Hα chemical shift patterns (*17*) suggests that a significant proportion of the assigned residues are involved in the formation of regular secondary structures (Figure 2). Indeed, a number of second-

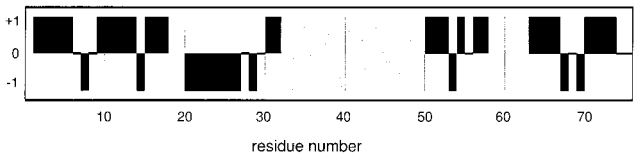

FIGURE 2: Chemical shift diagram of the Cα protons of HN76 according to the procedure of Wishart et al. (*17*). Deviations from the random coil chemical shifts are indicated by bars if they exceed a value of ±0.1 ppm.

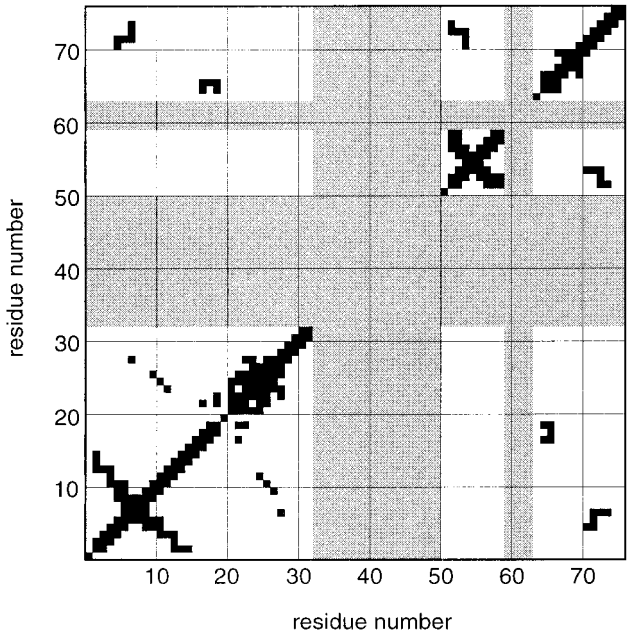

FIGURE 3: Interresidue NOEs identified in HN76. One square was generated for each (*i*, *j*) pair of residues displaying NOE connectivities with each other. The gray areas correspond to amino acids showing no connectivities.

ary structure elements can be derived from the NOE connectivities (Figures 1, 3, and 4). The Lys21−Ile28 segment displays strong NN (*i*,*i*+1), weak NN (*i*,*i*+2), and weak to medium αN (*i*,*i*+1 to *i*,*i*+4) interactions characteristic of an α helix (Figure 1). Four segments, Lys2−Ile6 (A), Val9−Glu15 (B), Glu52−Glu54 (C), and Ile71−Thr74 (D), display weak NN (*i*,*i*+1) and strong αN (*i*,*i*+1) connectivities characteristic of β strands. Long-range connectivities show that these four strands form a β sheet with B and D antiparallel to A, and C antiparallel to D (Figures 3 and 4). Other secondary structures include a type I turn (Asn7−Gly8) and two loops (Gly55−Leu58 and Glu67−Met70). The latter loop might in fact be helical, as suggested by its NOE connectivities (Figure 1) and by the chemical shifts of its Cα protons (Figure 2). These secondary structure assignments are further supported by the presence of slowly exchangeable protons (Figure 1).

Tertiary Structure. A number of interresidue NOE connectivities provide evidence for the presence of a four-stranded β sheet (see above, Figure 4). Other connectivities (Figure 3) reveal that the Lys21−Ile28 α helix interacts with several residues. Starting from its N terminus, the contacts involve Phe22 and Ala23 with Thr17 and Ile19, then Asp25, Asn26, and Asn27 with three residues belonging to β strand B (Asn12, Phe11, and Gln10), and finally Ile28 with Asn7, which belongs to the turn connecting strands A and B. The aromatic proton resonances of Phe11, unlike those of Phe22, are inequivalent, suggesting that this aromatic ring is immobilized between the α helix and strand A, according to the available NOE connectivities. These data suggest a close association of the α helix and of strands A and B, with the helix running roughly parallel to A and antiparallel to B. Additional interactions are observed between β strand C (Glu52−Glu54) and the Gly55−Leu58 loop. Several connectivities also indicate contacts between the loop connecting strand B and the α helix (Thr17−Ile19), and the Leu65−Ile66 segment (table in the Supporting Information). Some of the slowly exchangeable protons occur in these interacting regions (see above). Collectively, the NMR data have allowed the identification of a number of interactions among the secondary structure elements which amount to ca. 40% of the sequence, as well as with less structured parts of the protein. These data, together with the obligation for the polypeptide chain to position the four cysteine ligands (residues 34, 46, 49, and 62) around the [2Fe-2S] cluster, impose folding constraints that will be discussed below in relation with known structures.

Comparison with Plant- and Mammalian-Type Ferredoxins. The HN76 domain of *C. pasteurianum* hydrogenase has been shown to contain a [2Fe-2S] cluster with four cysteine ligands (*5*). Sequence similarity searches have revealed significant relationships only (not mentioning other hydro-

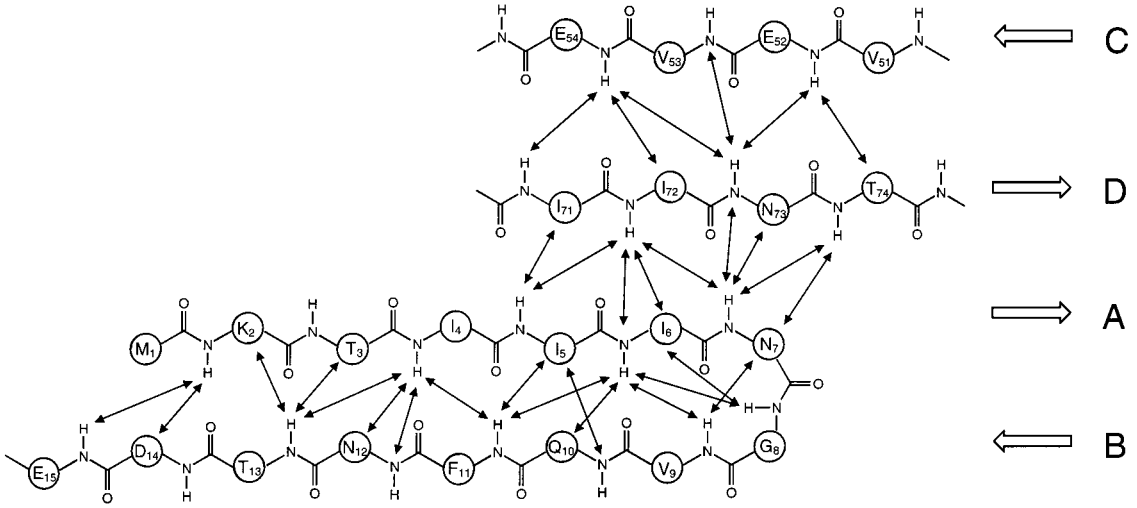

FIGURE 4: β sheet identified by long-range interresidue NOEs. The labeling of the β strands is described in the text.

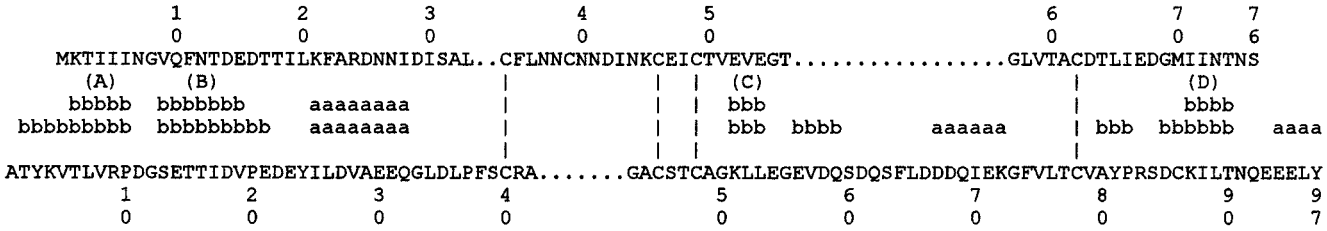

FIGURE 5: Sequence alignment of HN76 (upper line) and *S. elongatus* ferredoxin (lower line), based on secondary structure elements derived from 2D NMR data and on the cysteine ligands of the [2Fe-2S] cluster. Secondary structures for each protein are denoted in the central lines (a is α helix and b β strand). The β strands of HN76 are labeled with capital letters. *S. elongatus* Fd data were taken from ref *15*.

genases) with α subunits of formate dehydrogenases and with NuoG subunits of NADH−ubiquinone oxidoreductases (*5*), both of which have unknown three-dimensional structures. There are only two kinds of structurally characterized protein folds that accommodate all-cysteine ligated [2Fe-2S] clusters. The better known is that of numerous plant- and mammalian-type ferredoxins (Fd) (*18*). The other one has so far been found only once, in one of the two [2Fe-2S]-containing domains of the aldehyde oxidoreductase from *Desulfovibrio gigas* (*19*). This latter domain is a four-helix bundle, a structure that is clearly incompatible with the NMR properties of the HN76 domain described above. In contrast, at least some of the NMR-derived structural features of the HN76 domain are reminiscent of the structural framework of plant- and mammalian-type Fd as determined by X-ray crystallography (*20*−*23*) and to some extent by 2D NMR (*11*−*15*, *24*, *25*). A more detailed discussion of the similarities and differences between these proteins is therefore developed below.

The four-stranded β sheet and the α helix contacting two (A and B, see above) of these strands constitute a structural motif (hereafter called the β2αβ2 motif) which is very similar to the part of plant- and mammalian-type Fds that is farthest from the [2Fe-2S] cluster. The ^{1}H NMR resonances which are assigned to this part of HN76 display no paramagnetic interactions, and thus, the β2αβ2 motif is very likely to be distant from the [2Fe-2S] cluster in the HN76 structure as well. A mandatory common feature of the two proteins is the correspondence of the four cysteine ligands of the cluster. Of the five cysteine residues of HN76, Cys39 has previously been dismissed as a ligand on the basis of alignments with homologous proteins and also because the Cys39Ala variant had properties identical with those of the wild type (*5*). This near identity is now confirmed by the NMR data reported here. The sequence of HN76 has thus been aligned (Figure 5) with a plant-type Fd sequence by matching the segments belonging to the β2αβ2 motif and the cysteine ligands of the [2Fe-2S] cluster. This alignment based on established structural features highlights great similarities of the two proteins in the N-terminal (residues 1−35 of HN76) and in the C-terminal ends (residues 57−76 of HN76). In these regions of high similarity, HN76 differs slightly from plant-type Fds with a shorter pair of antiparallel strands (A and B) near the N terminus, a shorter loop (Asp29−Leu33) connecting the α helix to the first cysteine ligand, and the absence of the C-terminal helix. The relatively shorter Asp29−Leu33 loop in HN76 (four residues vs six in plant-type Fds) may account for the different orientation of the α helix. Indeed, whereas this helix runs across strands A and B in plant- and mammalian-type Fds (*11*−*15*, *20*−*25*), the NOE connectivities observed in HN76 indicate that the helix is roughly parallel to these two β strands (see above).

Significant discrepancies between the two proteins appear in the central region of the sequences. Whereas a short section including the second and third cysteine ligands and β strand C is conserved, HN76 differs from plant-type Fds in a seven-residue insertion (Asn37−Ile43) between the first and second cysteine ligands, and a 17-residue deletion between the third and fourth cysteine ligands (Figure 5). The seven-residue insertion is part of the Phe35−Lys45 segment for which only scant NMR data were obtained. It is therefore difficult to make inferences about its structure. However, the mere lack of sequential assignments suggests that this part of the protein folds closely around the paramagnetic [2Fe-2S] cluster. Indeed, on the basis of the plant Fd structural model (*15*, *20*−*22*), the position in HN76 of the seven-residue insertion could overlap the one occupied in plant Fd by residues 60−70, i.e., a portion of the sequence that is missing in HN76 (Figures 5 and 6). In this case, the Asn37−Ile43 insertion of HN76 would most likely be indispensable for the stability of the [2Fe-2S] cluster and of the protein altogether. The observation that the HN76 domain does not survive the deletion of the Asn37−Ile43 segment (M. Atta and J. Meyer, unpublished data) is in keeping with these predictions.

The Glu56−Lys72 section of *Synechococcus elongatus* Fd, for which there is no counterpart in HN76 (Figure 5), forms most of the left side of plant-type Fds as represented in Figure 6. This part of the structure could be partially substituted in the HN76 structure by the Asn37−Ile43 insertion (Figure 6). The Glu56−Lys72 segment of *S. elongatus* Fd includes a β strand (Glu56−Gln59) and an α helix (Asp67−Lys72) for which there are no signatures in the 2D NMR spectra of HN76, in agreement with the alignment proposed in Figure 5. In plant-type Fds, the Glu56−Gln59 strand forms a β sheet together with the Ala80−Arg83 strand (*15*). In HN76, the counterpart of the Glu56−Gln59 strand is missing, and accordingly, the counterpart of the Ala80−Arg83 strand, Thr64−Glu67, assumes no secondary structure, which again is in agreement with the alignment proposed in Figure 5. Another consequence of the 17-residue deletion in HN76 is the necessity for the polypeptide chain to fold back toward the [2Fe-2S] cluster after β strand C, which, according to the plant Fd model (*11*−*15*, *20*−*22*), runs away from the cluster. This is supported by the NMR data which show contacts between strand C (Glu52−Glu54) and the Gly55−Leu58 segment (see above). The contacts between the Thr17−Ile19 loop connecting strand B and the α helix, and the Leu65−Ile66 segment following the fourth cysteine ligand, are also features that have counterparts in the tertiary

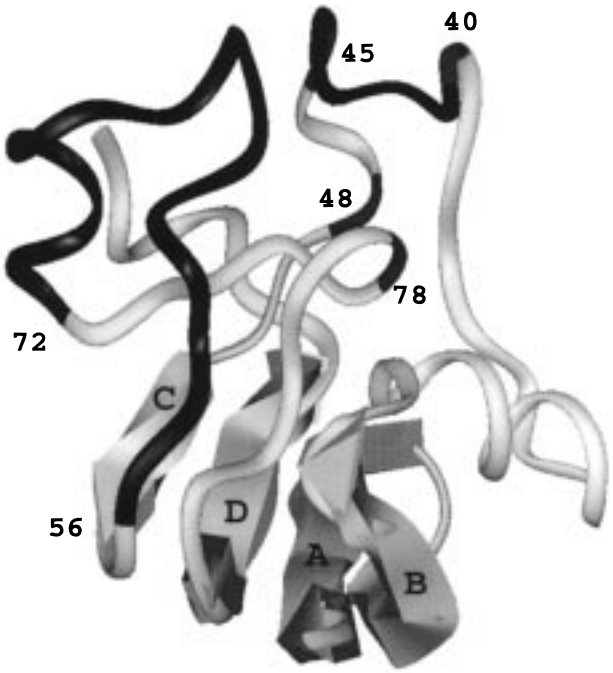

FIGURE 6: Scheme showing the similarities and differences between plant-type ferredoxins and the HN76 domain of *C. pasteurianum* hydrogenase. The structure represented is that of *S. elongatus* Fd (PDB entry 2CJN; *15*), using the INSIGHT II software from Molecular Simulations. The location of the [2Fe-2S] cluster in the upper-central part of the molecule can be derived from the positions on the main chain of its four cysteine ligands (dark gray parts of the main chain near numbers 40, 45, 48, and 78). The NMR data (see the text) and sequence alignment (Figure 5) indicate that the four-stranded (A−D) β sheet and the α helix are conserved in HN76, with minor variations. The latter would include a rotation of the α helix to make it more parallel to strands A and B, and a shorter connection between the helix (residues 25−32 in *S. elongatus* Fd and 21−28 in HN76) and the first ligand of the cluster (Cys40 in *S. elongatus* Fd and Cys34 in HN76; see Figure 5). In contrast, major differences are expected in the two black segments (residues 41−44 and 56−72). In NH76, the counterparts of residues 56−72 are missing (Figure 5), whereas the loop connecting the counterparts of cysteines 40 and 45 (34 and 46 in HN76, respectively) includes a seven-residue insertion (Figure 5). The scheme shows that these two regions are positioned in a way that would allow the longer ligand loop in HN76 to compensate in part for the deletion of the 56−72 segment.

structure of plant-type Fds. These data indicate that the two structures resemble each other not only in the $\beta2\alpha\beta2$ motif but also, to some extent at least, in the segments connecting this motif to the Fe−S cluster. Furthermore, even the general positioning of the [2Fe-2S] cluster and the arrangement of cysteine ligands around it might also be similar in the two structures, as previously inferred from circular dichroism and resonance Raman data (*5*). Indeed, the third (Cys49) and fourth (Cys62) ligands of HN76 must be nearer to the $\beta2\alpha\beta2$ motif than the two other cysteine ligands, because of their proximity to parts of the β sheet (Figure 5). It is also noted that the first and fourth cysteine ligands occur in relatively conserved regions of the sequences, and that the second and third cysteine ligands of both proteins are found in Cys-X-X-Cys runs followed by a short β strand belonging to the conserved β sheet (Figure 5). One may then envision a [2Fe-2S] cluster having one iron atom relatively buried and bound to the last two cysteines in the sequence, and the other iron atom nearer to the surface and bound to the two first cysteines in the sequence, in a fashion similar to that in plant-type ferredoxins (*11*−*15*, *20*−*22*). For the most part, the comparison made above between the structure of plant-type Fd and the folding proposed here for the HN76 domain can be extended to the recently determined structure of adrenodoxin (*23*). Here again, the main differences are observed in the part of the polypeptide chain linking the third and fourth cysteine ligands of the cluster (left side of the molecule in Figure 6). Interestingly, this region is also the one where plant- and mammalian-type Fds differ most (*23*). Indeed, the occurrence of 12, 29, and 36 residues between the third and fourth cysteine ligands of the cluster in HN76, plant-, mammalian-type Fd, respectively, is an interesting case of structural variation among otherwise similar proteins.

The well-structured C terminus of HN76 indicates that a reasonable estimation has been made for the junction between the N-terminal [2Fe-2S] domain and the remainder of the *C. pasteurianum* hydrogenase structure. According to secondary structure predictions (*5*), an α helix should occur shortly after residue 76 in *C. pasteurianum* hydrogenase. Whether this putative helix is the counterpart of the C-terminal helix of plant-type Fd remains to be established.

CONCLUSIONS

Despite the relatively small size (76 residues) of the hydrogenase N-terminal domain (HN76) and the large distance (ca. 8 Å) over which paramagnetic perturbations by the [2Fe-2S] cluster are detrimental to the collection of ^{1}H NMR data, a reasonable proportion of amino acid spin systems has been detected (75%) and sequentially assigned (70%). The data show that, as in plant- and mammalian-type Fds, the part of the structure that is farthest from the metal cluster displays a characteristic fold consisting of a four-stranded β sheet and an α helix ($\beta2\alpha\beta2$ motif). On the basis of these similarities, and taking into account the obligation to position the four cysteine ligands around the [2Fe-2S] cluster, we derived a sequence alignment of HN76 with plant-type Fds. This structure-based alignment, as well as NMR data affording tertiary structure information, suggests additional similarities in the connections of secondary structure elements to the cysteine ligands of the cluster. The main difference between the N-terminal domain of hydrogenase and plant- and mammalian-type Fds is a seven-residue insertion betwen the first and second cysteine ligands and a 17- or 24-residue deletion between the third and fourth cysteine ligands. Inspection of the plant-type Fd structure (*11*−*15*, *20*−*22*) and of the sequence alignment in Figure 5 suggests that in HN76 the insertion could compensate for the deletion as an insulator of the cluster from the solvent (Figure 6). In this case, the protein folds around the cluster might be similar in the three structures, despite the sequence discrepancies, as previously inferred from the near identity of the circular dichroism spectra of HN76 and of plant- and mammalian-type Fds (*5*).

Altogether, the data presented and discussed above provide strong support for the structural similarity of plant- and mammalian-type Fds with the N-terminal [2Fe-2S] cluster-containing domain of *C. pasteurianum* hydrogenase. Further downstream in the sequence of this enzyme, another domain is conspicuously homologous to, and therefore must fold in a fashion similar to that of, the well-known 2[4Fe-4S] ferredoxins (*26*). Ironically, it turns out that this archetypal

[Fe]-hydrogenase (*27*) includes two domains similar to each of the two first characterized ferredoxins, those from *C. pasteurianum* (*28*) and from spinach (*29*).

The N-terminal domain of *C. pasteurianum* hydrogenase had previously been observed, on the basis of high degrees of sequence similarity, to be homologous to several proteins or domains found in various hydrogenases, in formate dehydrogenase, and in complex I of aerobic respiratory chains. The structural data brought forth in this report demonstrate that all of these proteins or fragments thereof have folds similar to that of plant- and mammalian-type ferredoxins. This fold, which is thus found in organisms as diverse as anaerobic bacteria, phototrophs, aerobic bacteria, and eukaryotes, may therefore become a valuable thread for tracing the evolution of bioenergetic machineries.

SUPPORTING INFORMATION AVAILABLE

A table giving the proton chemical shifts at 293 K and pH 7.5 for the C39A variant of the HN76 protein. This material is available free of charge via the Internet at http://pubs.acs.org.

REFERENCES

1. Voordouw, G., and Brenner, S. (1985) *Eur. J. Biochem. 148*, 515−520.
2. Meyer, J., and Gagnon, J. (1991) *Biochemistry 30*, 9697−9704.
3. Malki, S., Saimmaime, I., De Luca, G., Rousset, M., Dermoun, Z., and Belaich, J.-P. (1995) *J. Bacteriol. 177*, 2628−2636.
4. Bui, E. T. N., and Johnson, P. J. (1996) *Mol. Biochem. Parasitol. 76*, 305−310.
5. Atta, M., Lafferty, M. E., Johnson, M. K., Gaillard, J., and Meyer, J. (1998) *Biochemistry 37*, 15974−15980.
6. Huber, J. G., Gaillard, J., and Moulis, J.-M. (1995) *Biochemistry 34*, 194−205.
7. Bax, A., and Davis, D. G. (1985) *J. Magn. Reson. 65*, 355−360.
8. Macura, S., Hyang, Y., Suter, D., and Ernst, R. R. (1981) *J. Magn. Reson. 43*, 259−281.
9. States, D. J., Haberkorn, R. A., and Ruben, D. J. (1982) *J. Magn. Reson. 48*, 286−298.
10. Wüthrich, K. (1986) *NMR of proteins and nucleic acids*, John Wiley, New York.
11. Oh, B.-H., and Markley, J. L. (1990) *Biochemistry 29*, 3993−4004.
12. Pochapsky, T. C., and Ye, X. M. (1991) *Biochemistry 30*, 3850−3856.
13. Lelong, C., Sétif, P., Bottin, H., André, F., and Neumann, J.-M. (1995) *Biochemistry 34*, 14462−14473.
14. Baumann, B., Sticht, H., Schärpf, M., Sutter, M., Haehnel, W., and Rösch, P. (1996) *Biochemistry 35*, 12831−12841.
15. Hatanaka, H., Tanimura, R., Katoh, S., and Inagaki, F. (1997) *J. Mol. Biol. 268*, 922−933.
16. Skjeldahl, L., Westler, W. M., and Markley, J. L. (1990) *Arch. Biochem. Biophys. 278*, 482−485.
17. Wishart, D. S., Sykes, B. D., and Richards, F. M. (1992) *Biochemistry 31*, 1647−1651.
18. Matsubara, H., and Saeki, K. (1992) *Adv. Inorg. Chem. 38*, 223−280.
19. Romão, M. J., Archer, M., Moura, I., Moura, J. J. G., LeGall, J., Engh, R., Schneider, M., Hof, P., and Huber, R. (1995) *Science 270*, 1170−1176.
20. Rypniewski, W. R., Breiter, D. R., Benning, M. M., Wesenberg, G., Oh, B.-H., Markley, J. L., Rayment, I., and Holden, H. M. (1991) *Biochemistry 30*, 4126−4131.
21. Ikemizu, S., Bando, M., Sato, T., Morimoto, Y., Tsukihara, T., and Fukuyama, K. (1994) *Acta Crystallogr. D50*, 167−174.
22. Fukuyama, K., Ueki, N., Nakamura, H., Tsukihara, T., and Matsubara, H. (1995) *J. Biochem. 117*, 1017−1023.
23. Müller, A., Müller, J. J., Muller, Y. A., Uhlmann, H., Bernhardt, R., and Heinemann, U. (1998) *Structure 6*, 269−280.
24. Miura, S., and Ichikawa, Y. (1991) *Eur. J. Biochem. 197*, 747−757.
25. Chae, Y. K., Abildgaard, F., Mooberry, E. S., and Markley, J. L. (1994) *Biochemistry 33*, 3287−3295.
26. Moulis, J.-M., Sieker, L. C., Wilson, K. W., and Dauter, Z. (1996) *Protein Sci. 5*, 1765−1775.
27. Chen, J.-S., and Mortenson, L. E. (1974) *Biochim. Biophys. Acta 371*, 283−298.
28. Mortenson, L. E., Valentine, R. C., and Carnahan, J. E. (1962) *Biochem. Biophys. Res. Commun. 7*, 448−452.
29. Tagawa, K., and Arnon, D. I. (1962) *Nature 195*, 537−543.

BI982416J